WARWICK
THE UNIVERSITY OF WARWICK

Manuscript version: Author's Accepted Manuscript
The version presented in WRAP is the author's accepted manuscript and may differ from the published version or Version of Record.

Persistent WRAP URL:
http://wrap.warwick.ac.uk/114960

How to cite:
Please refer to published version for the most recent bibliographic citation information. If a published version is known of, the repository item page linked to above, will contain details on accessing it.

Copyright and reuse:
The Warwick Research Archive Portal (WRAP) makes this work by researchers of the University of Warwick available open access under the following conditions.

Copyright © and all moral rights to the version of the paper presented here belong to the individual author(s) and/or other copyright owners. To the extent reasonable and practicable the material made available in WRAP has been checked for eligibility before being made available.

Copies of full items can be used for personal research or study, educational, or not-for-profit purposes without prior permission or charge. Provided that the authors, title and full bibliographic details are credited, a hyperlink and/or URL is given for the original metadata page and the content is not changed in any way.

Publisher's statement:
Please refer to the repository item page, publisher's statement section, for further information.

For more information, please contact the WRAP Team at: wrap@warwick.ac.uk.

warwick.ac.uk/lib-publications

Garcia, R., Sullivan, T. J., & Corte, G. D. (2010). Development of a displacement-based design method for steel frame-RC wall buildings. Journal of Earthquake Engineering, 14(2), 252-277. http://dx.doi.org/10.1080/13632460902995138

DEVELOPMENT OF A DISPLACEMENT BASED DESIGN METHOD FOR STEEL FRAME-RC WALL BUILDINGS

Reyes Garcia[1*], Timothy J. Sullivan[2], Gaetano Della Corte[3]

[1] MEEES Graduate Student, ROSE School, Italy. Current PhD Scholar, Dept. of Civil and Structural Engineering, University of Sheffield, UK. *Corresponding author: r.garcia@sheffield.ac.uk.
[2] Assistant Professor, Dept. of Structural Mechanics, University of Pavia, Italy.
[3] Assistant Professor, Dept. of Structural Engineering, University of Naples "Federico II", Italy.

Abstract

A Displacement-Based Design (DBD) methodology for steel frame-RC wall structures has been proposed. The effectiveness of the methodology in limiting lateral displacements has been tested by designing a set of case studies. Their structural performance was investigated through nonlinear time-history analyses by using seven spectrum-compatible accelerograms. For the seismic intensity and modelling assumptions considered in this work, it is found that the proposed design methodology controls the lateral displacements of the buildings well.

Keywords: displacement based design, steel frame-RC wall buildings, drift, displacement, time-history analyses

1. Introduction

During the last years, seismic design of structures has experienced a re-evaluation due to the introduction of new seismic design methodologies. Among them, Direct Displacement-Based Design (DDBD) has demonstrated its effectiveness in controlling structural displacements thus controlling the likely structural damage [Priestley *et al*, 2007]. More emphasis has been focused, however, toward the design methods for reinforced concrete (RC) structures, whereas less research effort has been directed to more complex systems such as frame-wall

buildings. To address this issue, Sullivan *et al* [2006] developed an innovative DBD methodology for regular RC frame-wall buildings, being also applicable to structures combining steel frame-RC wall structures. Having this in mind, the main scope of this work is to test the effectiveness of the new methodology in terms of displacement control in steel frame-RC wall buildings. To achieve this, a set of case studies are designed with the proposed methodology, and their structural performance is verified through time-history analyses.

1.1. *Features of frame-wall structures*

Frame-wall systems (also called hybrid or dual systems) are an attractive solution in high seismicity regions. In fact, they combine the structural advantages of frames and walls. One of these advantages is that walls provide good lateral stiffness to help control displacements over lower storeys and resist the seismic load. Even more, due to the intrinsic characteristics of functionality and service, layouts of buildings are usually required to include walls to form stair wells and lift shafts, being then convenient to use them also as earthquake resistant members. Frames offer additional energy dissipation and are particularly effective in controlling the deformations of upper storeys. Additionally, thanks to the interaction between frames and walls, smaller shapes can be used for steel beams and columns in dual systems than in bare moment resisting frames, with consequent economic savings.

Despite the fact that significant research efforts have been focused on the experimental and analytical performance of frame-wall systems, current seismic provisions include rather limited design guidelines for those structures [Sullivan *et al*, 2006]. A general drawback of current seismic design methodologies is that they are force-based, implying that they incorporate irrational design decisions and do not effectively control damage, as well documented by Priestley [Priestley, 2003; Priestley *et al*, 2007]. One specific issue ignored

by current design methods is that floor diaphragms impose displacement compatibility between frames and walls. An arbitrary assignment of ductility factors by means of force-reduction factors (as suggested by the codes) does not satisfy the displacement compatibility requirement. Actually, to achieve the same displacement, walls of typical dual systems are likely to undergo a much larger ductility demand than frames because of their smaller value of yield displacement [Sullivan *et al*, 2006].

In the context of this research, it is also worth pointing out that while the use of concrete and steel lateral load resisting systems together in construction is not common, there are situations in which it will be desirable to do so. Direct DBD has been shown to perform effectively for RC frame-wall systems [Sullivan *et al*, 2006] and while steel frame-RC wall systems should behave similarly, the influence of the different hysteretic properties of steel frames on the performance of the design methodology needs to be investigated.

2. Fundamentals of DDBD

In the last years, Direct Displacement Based Design (DDBD) emerged as a rational procedure for seismic design of buildings and bridges as an attempt to mitigate current design deficiencies [Priestley *et al*, 2007]. The design methodology has gained popularity and its principles, although described here for frame-wall structures, are equally applicable to other structural systems.

A major feature of the DDBD method is that whilst current force-based design methods characterise the structure by its elastic properties, the DDBD method uses the substitute structure approach [Shibata and Sozen, 1976] and characterises the structure by a single degree of freedom (SDOF) system with effective mass m_e, effective height h_e (Fig. 1a), and secant stiffness K_e, at the maximum response Δ_d (Fig. 1b). The maximum or design displacement Δ_d can be set by a displaced shape scaled to reach a design drift, θ_d, chosen to

ensure acceptable levels of damage for a given risk event. Once the displaced profile of the structure at the maximum displacement is known, the equivalent SDOF design displacement at the effective height, h_e, is defined by:

$$\Delta_d = \sum_{i=1}^{N}\left(m_i\Delta_i^2\right)\Big/\sum_{i=1}^{N}\left(m_i\Delta_i\right) \quad (1)$$

Where N is the total number of storeys, m_i is the storey mass, and Δ_i is the design displacement for the storey i. The effective height is also a function of the displaced shape of the masses at maximum response, in addition to the storey height h_i, and is calculated according to Eq. (2).

$$h_e = \sum_{i=1}^{N}\left(m_i\Delta_i h_i\right)\Big/\sum_{i=1}^{N}\left(m_i\Delta_i\right) \quad (2)$$

To calculate the effective mass of the system, m_e, the participation of the fundamental mode of vibration at maximum response is considered. The effective mass can be estimated by using Eq. (3).

$$m_e = \sum_{i=1}^{N}\left(m_i\Delta_i\right)/\Delta_d \quad (3)$$

Since the actual response of a structure subject to intense seismic actions is predominately non-linear, the effect of energy dissipation in the system is considered in the DDBD methodology through an equivalent viscous damping coefficient, ξ_{SDOF}, which includes both elastic and hysteretic damping components. Grant *et al* [2005] suggested that the amount of equivalent viscous damping is also dependent on the effective period of the substitute structure T_e as will be discussed in Section 3.4. Observe in Fig.1(c) that for the same level of ductility demand the level of equivalent damping assigned to a steel frame building possessing compact sections is higher than that of a RC frame building. This is a consequence

of the larger capacity of steel sections to dissipate hysteretic energy through more stable hysteresis loops during the nonlinear response of the structure.

The expected displacement ductility demand of the equivalent SDOF system, μ_Δ, can be calculated with Eq. (4).

$$\mu_\Delta = \frac{\Delta_d}{\Delta_y} \tag{4}$$

Where Δ_y is the yield displacement of the SDOF system (Fig. 1b) and is a function of the yield curvature, ϕ_y, of the structural sections. Detailed information about the calculation of Δ_y for frame-wall systems is given in Section 3.2.

Having established the design displacement of the equivalent SDOF system, and the corresponding expected damping, $\xi_{expected}$, for the expected displacement ductility demand, the effective period T_e can be read from a displacement spectrum appropriate for the level of equivalent viscous damping (Fig. 1d). In this work, displacement spectra associated with a damping different from 5% are calculated based on Eq. (5) provided by the Eurocode 8 (EC8) [CEN, 2003].

$$\eta = \sqrt{10/(5+\xi)} \geq 0.55 \tag{5}$$

The period T of a SDOF system is defined in terms of its mass M and stiffness K by:

$$T = 2\pi\sqrt{\frac{M}{K}} \tag{6}$$

By inverting Eq. (6), the effective stiffness, K_e, of the equivalent SDOF system at the design displacement can be estimated by:

$$K_e = 4\pi^2 m_e / T_e^2 \tag{7}$$

Finally, the design base shear, V_b, is given by Eq. (8).

$$F_d = V_b = K_e \Delta_d \tag{8}$$

The shear force V_b can be distributed over the height of the building as a function of the mass m_i, and the design displacement Δ_i of each storey. Thus, the corresponding force for the storey i can be defined by:

$$F_i = V_b \left(m_i \Delta_i \right) \Big/ \sum_{i=1}^{N} \left(m_i \Delta_i \right) \tag{9}$$

The forces provided by the latter equation are used to analyse the building and determine the flexural strength at the desired hinge locations. The design concepts in the Direct DBD approach are simple and clear. The major complexity lies in determining the substitute structure characteristics, the design displacement and the development of the design displacement spectra. The design method proposed in this paper uses this Direct DBD procedure to obtain the design forces, as outlined next. In particular, the next section demonstrates how the design displacement profile and equivalent viscous damping of the dual systems can be established as a function of strength assignments.

3. Proposed DDBD methodology for steel frame-RC wall buildings

The flowchart describing the proposed design method for dual steel frame-RC wall systems is depicted in Fig. 2. The several steps involved in the process are outlined in the following sections.

3.1. *Strength assignment*

A characteristic feature of the design methodology is that strength proportions are assigned at the start of the process (Fig. 2) by setting the proportion of base shear carried by frames and walls, in addition to the relative strength distribution of yielding elements within the frames [Sullivan *et al*, 2006]. Knowledge of the strength proportions can provide the expected displaced shape which is required to obtain the equivalent SDOF system characteristics.

Firstly, a plastic mechanism must be selected, and for this purpose, a weak beam-strong column approach is adopted. Although some codes allow the use of a weak column-strong beam mechanism for structures stabilised by a wall, this case is not considered here. Indeed, one main advantage of using walls is that they can protect from the formation of column-sway mechanisms. The design method could account for alternative mechanisms in prediction of the likely frame shear profile and subsequently in setting the wall inflection height, but this was deemed outside the scope of this work.

Having established the strength proportions, the shear profile over the height can be computed as explained below. This shear profile is then used to calculate the moment profile in the walls and the inflection height (h_{inf}, see Fig. 3), which will be needed for the calculation of both the design and the yield displacement profile (Sections 3.2 and 3.3).

In order to obtain the frame shear profile, the relative strength distribution of yielding elements within the frames is used. In this research, beams of equal strength for the full height of the structure were selected since they represent an attractive solution for design and construction purposes of dual systems [Paulay, 2002]. Indeed, the simplification of the design and construction processes is foreseen to reduce the construction costs because connection details would be standardised up the building height. However, it is worth mentioning that the uniform distribution may not be the most appropriate in cases where (i) the ultimate limit state gravity-load combination governs the design of the steel frame and (ii) significant differences between gravity loads are found at different floors. Note that the proposed design procedure is not constrained to the assumption of a uniform beam strength distribution and the designer can choose whatever alternative beam strength distribution s/he prefers.

Assuming that beam moments are carried equally by columns above and below a beam-column joint, the frame story shear can be obtained as a function of the beam strength:

$$V_{i,frame} = \frac{(\sum M_{b,i} + \sum M_{b,i\text{-}1})}{2(h_i - h_{i\text{-}1})} \quad (10)$$

Where $V_{i,frame}$ is the frame shear at level i, $M_{b,i}$ and $M_{b,i\text{-}1}$ are the beam strengths at levels i and i-1, and h_i and $h_{i\text{-}1}$ are the storey heights of levels i and i-1 measured from the base of the frame. Although the actual proportion of beam moments carried by the columns above and below the joint may not be equal, this approximation was shown to be suitable for the design of RC frame-wall structures by Sullivan *et al* [2006]. It is noteworthy that if constant beam strengths are used over the height of the structure, the frame shears are relatively constant with height, as indicated in Fig. 3 (higher shears should be expected at top and bottom storeys but the difference can typically be conservatively neglected). Note also that this assumption is valid for design to a damage control limit state in which frame yielding is expected to occur. Although the beam strengths are not actually known to begin with, Eq. (10) is useful as it enables the frame storey shear profile to be established up the height of the building.

To estimate the total wall 1st mode shear forces as a function of height, a triangular distribution of the fundamental mode of inertia forces up the height of the building is assumed. Accordingly, the total shear for storey i, $V_{i,total}$, can then be obtained as a proportion of the total base shear through Eq. (11) [Sullivan *et al*, 2006].

$$\frac{V_{i,total}}{V_b} = 1 - \frac{i}{n}\frac{(i\text{-}1)}{(n+1)} \quad (11)$$

Where n is the total number of storeys. For the case study structures, the use of a triangular distribution of inertia forces is correct when the displacement profile of the building is linear and the mass distribution is uniform. Although the design displacement profile is slightly non-linear, the approximation was found to be reasonably accurate by Sullivan *et al* [2006] for the purposes of setting the inflection height. Therefore, for the dual systems considered in

this research, the assumption of a triangular load distribution is considered sufficiently accurate for design purposes.

Because of equilibrium, wall shears can be obtained as the difference between the total base shear and the frame shear, as shown by Eq. (12).

$$\frac{V_{i,wall}}{V_b} = \frac{V_{i,total}}{V_b} - \frac{V_{i,frame}}{V_b} \tag{12}$$

Where V_b *is* the total base shear, $V_{i,wall}$ is the wall shear at level *i*, $V_{i,total}$ is the total shear at level *i*, and $V_{i,frame}$ is the frame shear at level *i*.

The frame shear proportions from Eq. (10) can be substituted into Eq. (12) so that the wall shear forces can be calculated as a function of the design base shear (Fig, 3, left). These wall shear forces are integrated over the height of the wall to compute the wall bending moment diagram and to establish the wall inflection height, h_{inf}, where the moment and curvature are both zero. The inflection height is required to set the expected displaced shape of the structure, as will become evident in the next section. In addition to the inflection height, the strength proportions also allow the calculation of the corresponding overturning proportions resisted by the frames and walls (see Fig. 3). These proportions of overturning moment are used later to estimate the damping of the equivalent SDOF system (Section 3.4).

3.2. *Yield deformation of walls and frames*

Because walls tend to control the displacement response of the structure, wall yield curvature is an important parameter for the development of the design displacement profile. The yield curvature of a rectangular wall, ϕ_{yWall}, can be obtained using the yield strain of the flexural reinforcement, ε_y, and the wall length, L_w, according to Priestley *et al* [2007]:

$$\phi_{yWall} = 2.00\varepsilon_y / L_w \tag{13}$$

The design displacement profile at yield of the wall, Δ_y, can then be established using the inflection height, h_{inf}, (see Fig. 3) and the height at the storey of interest h_i, in accordance with the appropriate version of Eq. (14) [Sullivan *et al*, 2006]:

$$\Delta_{iy} = \frac{\phi_{yWall} h_{inf} h_i}{2} - \frac{\phi_{yWall} h_{inf}^2}{6}, \text{ for } h_i \geq h_{inf} \tag{14a}$$

$$\Delta_{iy} = \frac{\phi_{yWall} h_i^2}{2} - \frac{\phi_{yWall} h_i^3}{6h_{inf}}, \text{ for } h_i < h_{inf} \tag{14b}$$

The frame ductility demand is used to provide an indication of the energy absorbed during the hysteretic response. Several expressions for the yield drift of steel frames exist in the literature [Gupta and Krawinkler, 2002; Paulay, 2003; Della Corte, 2006; Priestley *et al*, 2007]. Most of these equations are depth-dependant, and their use in the context of the displacement based design would introduce an iterative analysis. In order to avoid a time-consuming iterative design procedure, Sullivan *et al* [2006] proposed a simplified expression to evaluate the yield drift of a steel frame wherein the steel section yield curvatures are based on the ratio of the plastic modulus, *Z*, to the moment of inertia, *I*, as shown in Eq. (15). The authors observed that for AISC steel shapes, the trend of the relationship between *Z* and *I* for each steel group is practically constant, and therefore the nominal yield curvature of each group can be considered as constant as well (Table 1):

$$\phi_y = \frac{Z f_n}{EI} = \frac{Z}{I} \varepsilon_y \tag{15}$$

After some calibration with limited analytical data, Eq. (16) was proposed [Garcia, 2007] and used in this work to calculate the yield drift of steel frames.

$$\theta_{ySteelFrame} = \frac{\phi_{y,beam} L_b + 0.9(\phi_{y,col} h_{col})}{6} \tag{16}$$

Where L_b is the beam (or bay) length and h_{col} is the column (inter-storey) height. $\phi_{y,beam}$ and $\phi_{y,col}$ are the beam and column nominal yield curvature. The second addend in Eq. (16) takes into account deformability sources other than the beams in flexure (i.e. columns and beam-column panel zones). The coefficient 0.9 is the result of the calibration process in which the yield drift expression was matched to that obtained using the idealised non-linear static response of code-compliant moment frames that developed beam-sway mechanisms. As such, Eq.(16) has not been calibrated against experimental data from real structures and therefore future research should verify its full applicability. Adoption of Eq. (16) is proposed mainly due to i) its simplicity and ii) it does not require knowledge of the exact steel sections at the start of the design process, which avoids a time-consuming iterative design. When compared with arguably more accurate depth-dependant expressions of Gupta and Krawlinkler [2002] or the simplified expression of Priestley *et al* [2007], Eq. (16) slightly underestimates the value of yield drift by about 10-15% [Garcia, 2007]. Despite the additional research that should be done in this area, it is important to note that the displaced shape of frame-wall structures is controlled principally by the curvature profile in the walls [Sullivan *et al*, 2007] and that the role of the yield drift expression within the DBD methodology is principally to provide an estimate of the equivalent viscous damping offered by the frames (see Section 3.4).

It is worth mentioning that the selection of a steel shape based on a constant *Z*/*I* ratio cannot always be done directly. For instance, European steel groups (IPE and HE) possess a non linear variation of the plastic modulus *Z* vs. the moment of inertia *I* and are instead characterised by an almost constant value of the shape factor. In this case, the designer can select a beam depth and compute the yield curvature using Eq. (17) [Paulay, 2003].

$$\phi_y = 2.30\varepsilon_y / d_b \tag{17}$$

The required flexural strength will be known at the end of the design process, at which point the designer shall select the steel shape having the fixed depth and the plastic section modulus closest to the required value, checking the yield curvature assumed in design. With this in mind, it is clear that the proposed method is not only limited to be used along with AISC profiles, and the designer can alternatively adopt a different steel provider.

3.3. *Design displacement profile*

The design displacement shape depends on the design storey drift, θ_d, which can be initially taken as the code limit for non-structural damage. Nevertheless, Sullivan *et al* [2006] found that higher modes can have an important effect in tall structures, and proposed a reduction of the design drift for structures of up to 20 storeys in accordance with Eq. (18).

$$\theta_d = \theta_{d,limit}\left[1-\frac{(N-5)}{100}\left(\frac{M_{Frame}}{M_{Total}}+0.25\right)\right] \le \theta_{d,limit} \tag{18}$$

Where M_{Frame} and M_{Total} are the overturning resistance offered by the frame and the structure respectively, and N is the total number of storeys. The design drift may be reduced further if it is found that inelastic demands on walls and/or frames are likely to be excessive. For level i at height h_i, the design displacement Δ_i, is defined by [Sullivan *et al*, 2006]:

$$\Delta_i = \Delta_{iy} + \left(\theta_d - \frac{\phi_{yWall} h_{inf}}{2}\right)\cdot h_i \tag{19}$$

Once Δ_i is found, the design displacement and the characteristics of the substitute structure can be calculated using Eqs. (1) to (3).

3.4. *Design ductility values, effective period and equivalent viscous damping (DBD)*

As previously mentioned, energy dissipation in the building is represented by an equivalent viscous damping comprising an elastic and a hysteretic component. The hysteretic component

is a function of the expected ductility demand and the effective period of the substitute structure [Grant *et al*, 2005; Blandon and Priestley, 2006]. In order to use the equivalent viscous damping approach, the ductility demand on the walls should be calculated using the displacement at the effective height. Therefore, the wall displacement ductility demand, μ_{Wall}, can be defined as the design displacement divided by the yield displacement of the walls at the effective height, according to Eq. (20):

$$\mu_{Wall} = \frac{\Delta_d}{\Delta_{he,y}} \tag{20}$$

Where Δ_d is the design displacement calculated with Eq. (1) and $\Delta_{he,y}$ is the yield displacement of the wall at the effective height, obtained substituting the effective height into the appropriate version of Eq. (14). The displacement ductility demand on the frame at each level ($\mu_{Frame,i}$) up to the height of the building is defined by Eq. (21).

$$\mu_{Frame,i} = \left(\frac{\Delta_i - \Delta_{i\text{-}1}}{h_i - h_{i-1}} \right) \frac{1}{\theta_{ySteelFrame}} \tag{21}$$

Where Δ_i, $\Delta_{i\text{-}1}$, h_i and $h_{i\text{-}1}$ are the displacements and heights at levels *i* and *i*-1, respectively, and $\theta_{ySteelFrame}$ is the yield drift of the frame. If beams of equal strength are used up to the height of the structure, the ductility defined by Eq. (21) for each storey can be averaged to give the frame displacement ductility demand. Alternatively, if beams of different strength over the height of the structure and/or beams of different length at a given storey are used, the ductility demand for each storey should be calculated as the ratio of the storey drift to the storey yield drift associated with the average frame proportions for that storey. The weighted-average displacement ductility demand on the frame should then be obtained factoring storey ductility demands by resistance (i.e. work done).

The frame-wall system ductility demand is found by taking the average of the frame and wall ductility values, weighted by their overturning resistance proportions according to [Sullivan *et al*, 2006]:

$$\mu_{sys} = \frac{M_{Wall}\mu_{Wall} + M_{Frame}\mu_{Frame}}{M_{Wall} + M_{Frame}} \tag{22}$$

Where M_{Wall} and M_{Frame} are the wall and frame overturning resistance, and μ_{Wall} and μ_{Frame} are the displacement ductility demands for the wall and frame, respectively. This approach recognises that the lateral resistance offered by the frames and walls to the equivalent SDOF system is best gauged by the overturning resistance which, in contrast to the base shear, considers the lateral resistance offered by the frames and walls up the height of the structure.

Although the wall ductility demand given by Eq. (20) is appropriate for estimation of the equivalent viscous damping, it is not a good indicator of the inelastic deformation that the walls will undergo. A more appropriate parameter is the wall curvature ductility $\mu_{\phi Wall}$, which can be obtained in accordance with Eq. (23) [Sullivan *et al*, 2006]:

$$\mu_{\phi Wall} = 1 + \frac{1}{L_p \phi_{yWall}}\left(\theta_d - \frac{\phi_{yWall} h_{inf}}{2}\right) \tag{23}$$

Where L_p is the wall plastic hinge length, θ_d is the design storey drift, ϕ_{yWall} is the yield curvature of the walls, and h_{inf} is the inflection height. The wall plastic hinge length to be used in the latter equation can be taken as the maximum value given by Eq. (24).

$$L_p = 0.022 f_y d_b + 0.054 h_{inf} \tag{24a}$$

$$L_p = 0.2 L_w + 0.03 h_{inf} \tag{24b}$$

Where f_y is the yield stress (MPa), d_b the diameter of the longitudinal reinforcement in the wall, L_w is the wall length and h_{inf} is the inflection height. These two equations have been

adapted from Priestley [2003] with the inflection height substituting the total height. This is done to reflect the manner in which the plastic hinge length depends on the slope of the curvature profile and adopting the height to the point of inflection best matches the conditions under which the plastic hinge length expressions were developed (see Priestley *et al* [2007] for more details).

The curvature ductility capacity of a RC wall will depend on the strain limits selected for the concrete in compression, ε_c, and the longitudinal reinforcement in tension, ε_s. Assuming values of ε_c=0.018 and ε_s=0.06, Priestley and Kowalsky [1998] found that the ultimate curvature ϕ_u of a reinforced concrete wall is well represented by:

$$\phi_u = \frac{0.072}{L_w} \tag{25}$$

The latter equation in combination with Eq. (13) indicates that the wall curvature ductility capacity is approximately equal to:

$$\mu_{Wall,cap} = \frac{\phi_u}{\phi_y} = \frac{0.036}{\varepsilon_y} \tag{26}$$

If the checks on ductility indicate that the inelastic deformation associated with the design drift will be excessive (i.e. if $\mu_{\phi Wall} > \mu_{Wall,cap}$), then the design drift can be reduced and the design displacement profile recomputed. If the ductility demands are sustainable, then the next step in the design procedure is to compute equivalent viscous damping values. Frame ductility demands should also be limited. However, for typical frame proportions and non-structural storey drift limits, ductility demands on well detailed frames will not be critical and therefore an explicit check is not typically required.

Grant *et al* [2005] recommend that the hysteretic component of the equivalent viscous damping be computed as a function of the effective period, T_e. As T_e is unknown at the start

of the design process, a trial value can be used and an iterative design process adopted. A reasonable first trial value of the effective period $T_{e,trial}$, can be obtained for typical frame-wall structures by using Eq. (27) [Sullivan *et al*, 2006].

$$T_{e,trial} = \frac{N}{6}\sqrt{\mu_{sys}} \tag{27}$$

Where N is the total number of storeys and μ_{sys} is the system ductility (Eq. 22). For a steel beam with bi-linear hysteretic behaviour and RC walls with a Takeda hysteretic model, the equivalent viscous damping can be estimated by means of [Grant *et al*, 2005]:

$$\xi_{SteelFrame} = 5 + 16.1\left(1 - \frac{1}{\mu_{Frame}^{0.952}}\right)\left(1 + \frac{1}{(T_{e,trial} + 0.945)^{2.648}}\right) \tag{28}$$

$$\xi_{Wall} = 5 + 18.3\left(1 - \frac{1}{\mu_{Wall}^{0.588}}\right)\left(1 + \frac{1}{(T_{e,trial} + 0.848)^{3.607}}\right) \tag{29}$$

Damping of the equivalent SDOF system can be evaluated with Eq. (30) [Sullivan *et al*, 2006]:

$$\xi_{sys} = \frac{M_{Wall}\xi_{Wall} + M_{Frame}\xi_{Frame}}{M_{Wall} + M_{Frame}} \tag{30}$$

The next step is to develop the displacement spectrum at the design damping level given by Eq. (30), and read off the required effective period (Fig. 1d).

If the dependency of the equivalent viscous damping on the effective period is taken into account using Eqs. (28) and (29), a trial effective period must be first established and subsequently compared with the effective period read from the displacement spectrum. If they do not match, then the period obtained from the displacement spectrum replaces the trial period and the design step is repeated. When the trial period finally matches the period read from the displacement spectrum, the effective stiffness and design base shear can be calculated, and the required member design strengths can be established. However, since in

the design examples presented in this paper the dependency of the equivalent viscous damping on the effective period is negligible, the use of Eqs. (28) and (29) do not imply any need for iterations in the design process. It must be remarked that Priestley *et al* [2007] have proposed alternative approaches to completely eliminate the effective period dependency of the equivalent viscous damping.

With reference to Fig. 2, the last design step of the proposed method requires capacity design to avoid undesirable failure modes in structural members. Since the main goal of this work is to verify the effectiveness of the proposed design methodology in terms of drift control, and because capacity design is outside the scope of the research, the design process is continued only until wall, beam and column flexural strengths are obtained.

In this work gravity load combinations have not been explicitly considered as in regions of high seismicity they are not likely to be critical to member sizes. However, in regions of low and moderate seismicity, gravity load effects may become more significant. To address this issue in the DDBD approach, the gravity-load design could be undertaken to set initial frame member sizes. This gravity dominated frame strength distribution could then be directly considered in evaluating the shear profile and inflection height expected in the walls. With the wall inflection height known, the design displacement profile can be established and the design procedure outlined here followed as normal.

4. Performance of the proposed design methodology

4.1. *Case studies and design spectrum*

For verification purposes, the design method was applied to five regular buildings with 4, 8, 12, 16 and 20 storeys. In this paper the details and results of the 4, 12 and 20 storey structures are presented since these structures provide a reasonable representation of the performance of the methodology for all the case study structures. For information on the 8 and 16 storey case

studies refer to Garcia [2007]. The structures were assumed to be fixed at the base, having a lateral resistant system formed by two RC walls and two steel frames in each direction. It is also assumed that the intermediate framing shown in Fig. 4 utilises pinned connections that do not offer lateral resistance. The proposed layout is regular in plan and elevation (Fig. 4, left) and the general geometry of the buildings is presented in Table 2. Possible 3D effects have been ignored in the design methodology so that the structure can be idealised as a 2D model for analysis purposes.

The selected design spectrum corresponds to the EC8 [CEN, 2003] type 1 spectrum with soil type C. The peak ground acceleration used for the design is 0.5g. Fig. 5 shows the 5%-damped acceleration and displacement design spectra. Although EC8 uses a cut-off period of 2.0s, in this work it was decided to extrapolate the initial linear displacement spectrum in order to impose significant levels of seismic demand on taller structures. This has been done in recognition of the fact that the spectral displacement cut-off period is dependent on earthquake magnitude [Faccioli *et al*, 2004; Campbell and Bozorgnia, 2006] and it was desirable to consider whether the proposed methodology would be effective when utilised for taller structures in regions of high seismicity.

The material properties considered for the structures are, for concrete f'_c=30 MPa and E_c=25740 MPa, while for reinforcement and steel shapes (Grade 50) f_y=400 MPa and E_s=200000 MPa. Note that these are expected values of strength and stiffness, and therefore are not factored. The seismic weight of the concrete floors was calculated considering a concrete density of 24.5 kN/m^3 and a slab thickness of 200 mm. A super-imposed dead load of 1 kPa, a reduced live-load of 1 kPa and a loaded floor area of 982 m^2 at each level are also considered.

4.2. *Design of case studies*

For illustrative purposes, the proposed methodology is detailed for the design of the 12 storey building.

Step (1). Assign strength proportions and calculate wall inflection height. Beams of equal strength are used up to the height of the building. Base column strengths are assigned to provide an inflection height of 0.66 the inter-storey height (see Fig. 3, right). This is done to conservatively protect the top of the base columns against plastic hinging, although other strength proportions can be adopted to suit the designer. It is assumed that half of the beam moments of the first floor are distributed below the joints to the top of the ground storey columns (Eq. 12), and therefore the ground storey shear will be 1.5 times larger than the shear at other storeys. As a proportion of beam strengths, the flexural strengths at the base of the exterior and interior columns are therefore 100% and 200% the beam strength respectively.

Since shear proportions control the wall inflection height and therefore the wall curvature ductility demand, shear proportions on frames and walls are initially assigned so that Eq. (26) is satisfied. Note that by using a relatively large inflection height it may be that for a given storey drift limit the curvature ductility capacity of a wall is not being fully utilised, and the designer might choose to increase the shear proportion carried by the frames. On the other hand, if the inflection height is relatively low, then the design storey drift may have to be reduced in order to maintain a curvature ductility limit. Additionally, the design of the walls based on the assigned shear proportions must produce dimensions and steel reinforcement contents to satisfy the maximum and minimum requirements of the codes. This implies that the designer is free to choose the shear proportions to obtain the most suitable design solution. In this example, it is decided that walls resist $50\%V_b$ and therefore frames will resist

50%V_b. If the frame ground storey base shear is 1.5 times that of the rest of the stories, this means that 33.3%V_b will be resisted by the frames above the 1st floor. By knowing that each storey of the building has 12 beam ends and h_{col}=4 m, the beam strength (from Eq. 12) is:

$$M_b = 0.333V_b(4)/12 = 0.11V_b$$

Having established the shear proportions, it is possible to calculate the inflection height of the walls, h_{inf}, considering the overturning moments as a function of V_b (refer to Fig. 3, left). Fig. 6(right) shows the moment profiles for the whole building, where h_{inf} =30.83 m, M_{Frame}=17.33V_b, M_{Wall}=16.0 V_b and M_{Total}=33.33 V_b. The corresponding shear profiles from Eqs. (10) to (12) are shown in Fig. 6(left).

Step (2). Selection of beam group and calculation of yield drifts. A steel beam group can be initially selected in order to control deflections due to gravity loads or from experience. In this work it was decided to adopt a limit value of beam length to depth ratio equal to 15. Considering L_b=8 m, the proposed beam group depth is:

$$d_b = 8/15 = 0.53\text{m}$$

Therefore, a beam group of 530 mm (21” in the AISC charts) is selected for design. Columns in modern steel buildings are frequently built with 14” (355 mm) shapes. Furthermore, the wide availability of W14 shapes and plastic section modulus, *Z*, make them appropriate to be used as column sections. Note that while capacity design requirements could require larger column sizes over the lower floors, underestimating the column size implies yield deformations are overestimated, ductility and damping are conservatively underestimated and therefore the required design strengths are overestimated. The yield curvature of beam and column sections is calculated with Eq. (15) and the corresponding *Z*/*I* values given in Table 1.

For the beam (W21): $\phi_{y,beam} = (4.04)(0.002) = 0.00808$

For the column (W14): $\phi_{y,col} = (5.52)(0.002) = 0.01104$

The frame yield drift is (Eq. 16): $\theta_{ySteelFrame} = \dfrac{(0.00808)(8) + 0.9(0.01104)(4)}{6} = 0.0174$

The wall yield curvature is calculated using Eq. (13), $\phi_{yWall} = 2(0.002)/6 = 0.00066$.

Therefore, the displacement profile at yield of the wall, Δ_{iy}, can be established using the wall inflection height (Step 1) and the appropriate version of Eq. 14 (see column 3 of Table 3).

Step (3). Design displacement profile. A drift limit of 2.5%, intended to control damage of non-structural elements in the building, is selected for these case studies. The design drift is therefore computed using Eq. (18) and the overturning moments M_{Frame} and M_{Total}.

$$\theta_d = 0.025\left[1 - \frac{(12-5)}{100}\left(\frac{17.33}{33.33} + 0.25\right)\right] = 0.0236 < 0.025$$

The design displacement profile (Δ_i) calculated with Eq. (19) is shown in column 4 of Table 3.

Step (4). Perform the DDBD. Based on the results of columns 4, 5 and 6 of Table 3, it is possible to estimate the effective height, effective mass and design displacement of the equivalent SDOF (notice that the mass is considered as constant for all the storeys).

Eq. (1), $\Delta_d = 4.43/6.27 = 0.71\text{m}$

Eq. (2), $h_e = 214.25/6.27 = 34.19\text{m}$

Eq. (3), $m_e = 7250(6.27)/0.71(9.81) = 6557\text{T}$

Step (5). Verification of ductility demands on frames and walls.

(a) For the frame. Eq. (21) provides the ductility demand at each storey based on the drift values calculated with Δ_i (column 4, Table 3), h_{col}=4 m and $\theta_{ySteelFrame}$=0.0174. Results are presented in column 7 of Table 3. Because beams of equal strength are used, the frame displacement ductility demand equals the average displacement ductility demand of the 12 storeys:

$$\mu_{Frame} = 14.8/12 = 1.23$$

(b) For the wall. The approximate wall curvature ductility capacity (Eq. 26) is:

$$\mu_{Wall,cap} = 0.036/0.002 = 18.0$$

For this building $h_e > h_{inf}$, and therefore using Eq. (14a) the yield displacement at the effective height h_e is:

$$\Delta_y = \frac{(0.00067)(30.83)(34.19)}{2} - \frac{(0.00067)(30.83)^2}{6} = 0.25\text{m}$$

The wall design ductility (Eq. 4): $\mu_{\Delta,Wall} = 0.71/0.25 = 2.87$

Assuming a bar diameter of 24 mm, the length of plastic hinge is (Eq. 24):

$$L_p = 0.022(400)(0.024) + 0.054(30.83) = 1.87\text{m}$$

$$L_p = 0.2(6) + 0.03(30.83) = 2.12\text{m}\,(\text{Governs})$$

According to Eq. (23), the wall curvature ductility demand is:

$$\mu_{\phi Wall} = 1 + \frac{1}{(2.12)(0.00067)}\left(0.0236 - \frac{(0.00067)(30.83)}{2}\right) = 10.44 < 18.0 \ \text{(OK)}$$

From these results it follows that the design drift does not need to be reduced.

Step (6). Calculate equivalent viscous damping of frames and walls. Though the equivalent viscous damping is rigorously a function of the effective period (Eqs. 28 and 29), this dependency is actually very weak and for effective periods greater than 1s it can be neglected for design purposes. Therefore, the equivalent viscous damping can be calculated as a function of only the design ductility.

(a) For the frame: $\xi_{SteelFrame} = 5 + 16.1\left(1 - \frac{1}{(1.23)^{0.952}}\right) = 7.9\%$

(b) For the wall: $\xi_{Wall} = 5 + 18.3\left(1 - \frac{1}{(2.87)^{0.588}}\right) = 13.5\%$

(c) For the SDOF system: $\xi_{sys} = \frac{(16.0)(13.5) + (17.33)(7.9)}{16.0 + 17.33} = 10.6\%$

Step (7). Calculation of the effective period. The displacement design spectrum for ξ_{sys}=10.6% can be computed multiplying the spectral values of the 5% damping spectrum by the factor η.

Eq. (5), $\eta = \sqrt{10/(5 + 10.6)} = 0.80 > 0.55$

The displacement design spectrum for ξ_{sys}=10.6% used for the design is depicted in Fig. 7. Notice that for Δ_d=0.71 m, the calculated equivalent period T_e is approximately 4.1 s. At this stage, all the characteristics of the equivalent SDOF system have been calculated. Intermediate design results for the 12 storey structure are summarised in Table 4. Results for the other case studies have been obtained following the same procedure described in previous paragraphs.

Step (8). Determine effective stiffness and design base shear of the equivalent SDOF system.

Eq. (7), $K_e = 4(3.1416)^2(6557)/(4.1)^2 = 15250\text{kN/m}$

Eq. (8), $V_b = (15250)(0.71) = 10770\text{kN}$

Step (9). Beam and column strengths and wall moments.

(a) For the frame:
Beam strength, $M_b = 0.11(10770) = 1197\text{kNm}$

Interior column strength, $M_{col,int} = 2(1197) = 2366\text{kNm}$

Exterior column strength, $M_{col,ext} = 1197\text{kNm}$

Once design strengths for the beams and columns have been calculated, it is possible to choose steel sections from the shape group selected at the start of the design based on the plastic modulus and an estimate of the yield strength of the steel section. To consider the effects of post-yield stiffness for these case studies, the design strength is divided by a factor $[1+k(\mu_{Frame}-1)]$ to obtain the section yield strength, where k is the post-yield displacement stiffness (taken here as 5%). Hence, for the beam considered in this example:

$M_{y,b} = 1197/1.012 = 1183\text{kNm}$

Considering that $Z=M_n/f_y$, the beam section can be directly selected from the steel supplier charts. In this case, the AISC tables are used and therefore:

$Z = 1183/400\times10^3 = 0.003\text{m}^3 = 180\text{in}^3$ - Therefore, select a beam 21×73 (M_y=1130 kNm)

(b) For the walls (for one wall only): $M_{Wall} = 16.0V_b/2 = 8(10770) = 86164\text{kNm}$

The reinforcement estimates for the walls were obtained following the procedure suggested by Englekirk [2003]. Final design sections and longitudinal reinforcement of walls are included in Table 5. Notice that the flexural strength of steel beams and columns was selected to approximately match the flexural strength calculated in the DBD procedure. Wall longitudinal reinforcement ratios are between the maximum and minimum values suggested by Paulay and Priestley [1992]; hence, they are considered as realistic.

Step (10). In a full detailed design of a real structure, the final step is to perform capacity design (see Fig. 2). This step could be expected to increase column sizes but as noted in Step 2, such an increase can be conservatively ignored in the DDBD phase. Nevertheless, capacity design is outside the scope of this paper and therefore the design is considered complete for the purpose of this contribution. A thorough review of the issues related to capacity design can be found in Sullivan *et al* [2006].

4.3. *Time-history analysis of case studies*

The modelling for time history analyses of the case studies was performed in Ruaumoko [Carr, 2004]. Seven code-compatible artificial accelerograms generated by SIMQKE [Carr, 2004] were selected for the analyses so that they matched the design spectrum. Fig. 8 shows the displacement spectra for the seven records and their average demand for an elastic viscous damping level of 10%, as well as the average from the seven records compared to the design spectrum.

2D models of the structures were developed using Giberson beam elements [Carr, 2004]. The beams are modelled from column centreline to column centreline, which is consistent with the assumptions made in the design. The strength of members was set to match the design results. Floor systems are assumed to act as rigid diaphragms, and P-delta effects were not included in the verification analyses as they were not considered in the design process.

Recommendations to account for P-delta effects within a Direct DBD framework are provided by Priestley *et al* [2007]. Note that analyses by Sullivan *et al* [2006] indicated that P-delta effects are not typically significant for RC frame-wall structures of up to 20 storeys in height when the response drifts are smaller than the assumed design drift limits.

The hysteretic behaviour of walls was represented by the Takeda model [Carr, 2004] with 5% post-yield displacement stiffness and the unloading model of Emori and Schonbrich [1978]. Parameters for the Emori and Schonbrich model included an unloading stiffness factor of 0.5, together with a reloading stiffness factor of 0.0 and a reloading power factor of 1.0. Refer to the Ruaumoko manual [Carr, 2004] for further details. On the other hand, yielding steel beams and columns are modeled with a bi-linear hysteresis model with a 5% of post-yield displacement stiffness ignoring Bauschinger effects and without stiffness degradation. The post-yield displacement stiffness is dependent on the strain-hardening qualities of the steel, which tend to vary from manufacturer to manufacturer. The value of post-yield displacement stiffness adopted in this work is considered to be relatively large for steel structures and future work could look to consider the sensitivity of the results to lower values. The plastic hinge lengths associated with the RC wall were calculated using Eq. (24), whereas the plastic hinge length in the steel beams and columns was set equal to the section depth.

The models use effective section properties up until yield, obtained by taking the design strength divided by the yield curvature. An approximation for the yield curvature in walls was obtained from Eq. (13). Columns above the ground floor were modeled as elastic elements with their initial stiffness because they are not intended to yield. This implies that appropriate capacity design would have ensured that plastic activity is concentrated in regions associated with the intended collapse mechanism. Values for the moment of inertia of the

steel beams and columns were directly taken from the values provided by the AISC tables [AISC 2001].

Damping is modelled using a tangent stiffness Rayleigh damping model according to the recommendations of Priestley and Grant [2005]. Priestley and Grant [2005] provide a series of expressions to estimate the 1st mode damping so that the elastic damping of the 1st mode at maximum response of the MDOF system is effectively 5% of the critical damping. Consequently, 1st mode tangent stiffness damping values of 2.5, 3.3 and 3.7% are assigned to the 4, 12 and 20 storey buildings, respectively.

For analysis purposes, seismic loadings have been considered without combination with gravity loads as research by Pinto *et al* [1997] found that similar responses are obtained from nonlinear time-history analyses of structures designed with or without considering gravity loads. Additionally, Priestley *et al* [2007] have suggested that gravity loads play a minor role in the analyses and therefore their effects can be disregarded. However, as mentioned in Section 3.4, in regions of low and moderate seismicity gravity load effects may become more significant both for design and analysis.

4.4. *Evaluation of results from time-history analyses*

The effectiveness of the methodology can be evaluated by comparing the displacement response from time-history analysis with the target displacement shape selected for design. Since storey drift is an important parameter to identify potential damage, it is also critical to maintain maximum storey drifts below the limit drift set in the design process.

The results for the 4, 12 and 20 storey structures are presented in Figs. 9, 10 and 11. In the set of figures, the upper-left plots show the maximum absolute lateral displacement over the height of the building, whereas the upper-right plot presents the maximum absolute inter-

storey drifts. Lower plots allow a clear comparison between the average of these values and the target drifts and displacements considered during the design process. In this latter set of plots, drifts corresponding to the 1st mode refer to the original drift limit of 2.5% selected for design purposes, i.e. not reduced for higher mode effects (see step (3) at Section 3.4).

By comparing the average drift and displacement demands from time-history analyses with the values used in the design, it is evident that the design method works well for the various case study structures. Average drift demands are marginally lower than the design and limit values, indicating that the design method is efficient but also sufficiently conservative. The design drift reduction to account for the effect of higher modes has worked acceptably. Nevertheless, because Eq. (18) considers higher mode effects in an approximate manner, future research could improve the accuracy of the equation and the design methodology for taller structures. Note that while the recorded displacements and drifts appear low for the 20 storey structure, it is important to consider that at the effective period range of this structure, the accelerograms impose lower levels of demand than the design spectrum (see Fig. 8). As such, it is concluded that the DDBD method has performed well for the various case study structures investigated.

5. Summary and conclusions

A direct displacement-based design method for steel frame-RC wall structures has been proposed in this work. The effectiveness of the methodology has been tested by designing several case studies. Their structural performance has been verified through time-history analyses by using seven accelerograms compatible with the design spectrum from the EC8. For the ground motion intensity and modelling assumptions considered in this work, the design methodology effectively controlled the deformations and therefore likely damage of the case study buildings.

Acknowledgments

The first author wishes to thank the Erasmus Mundus Programme and MEEES Consortium for providing financial support during his period of study in ROSE School (Italy) and Joseph Fourier University of Grenoble (France).

References

AISC [2001] *Manual of Steel Construction, 3rd Edition*, American Institute of Steel Construction Inc., USA.

Blandon, C.A., Priestley, M.J.N. [2006] "Equivalent viscous damping equations for Direct Displacement-Based Design", *Journal of Earthquake Engineering*, **9**, Special Edition No. 2, 257-278.

Campbell KW, Bozorgnia Y. [2006] "Campbell-Bozorgnia NGA empirical ground motion model for the average horizontal component of PGA, PGV and SA at selected spectral periods from 0.01–10.0 seconds", *Interim Report for USGS Review*, May 2006.

Carr, A. [2004] *Ruaumoko 3D. A Program for Inelastic Time History Analysis*, Department of Civil Engineering, University of Canterbury, NZ.

CEN [2003] *Eurocode 8: Design of Structures for Earthquake Resistance*, Final Draft, Comité Européen de Normalisation, Brussels, Belgium.

Della Corte G. [2006] "Vibration mode vs. collapse mechanism control for steel frames", *Proceedings of the Fourth International Specialty Conference on Behaviour of Steel Structures in Seismic Areas (STESSA 2006)*, Yokohama, Japan, pp. 423-428.

Emori, K., Schonbrich, W.C. [1978] "Analysis of reinforced concrete frame-wall structures for strong motion earthquakes", *Civil Engineering Studies*, Structural Research Series, No. 434, University of Illinois, Urbana, USA.

Englekirk R.E. [2003] *Seismic Design Of Reinforced And Precast Concrete Buildings*, John Wiley And Sons, New York, USA.

Faccioli E, Paolucci R, Rey J. [2004] "Displacement spectra for long periods", *Earthquake Spectra*; **20**(2), 347–376.

Garcia, R, [2007] "Development of a displacement based design method for steel frame-RC wall buildings", MSc Dissertation, ROSE School, University of Pavia, Italy.

Grant, D.N., Blandon, C.A., Priestley, M.J.N. [2005] *Modelling Inelastic Response in Direct Displacement-Based Design*, Research report No. ROSE-2005/03, IUSS Press, Pavia, Italy.

Gupta, A., Krawinkler, H. [2002] "Relating the seismic drift demands of SMRFs to element deformation demands", *Engineering Journal*, Second Quarter, 100-108.

Paulay, T. [2002] "A displacement-focused seismic design of mixed building systems", *Earthquake Spectra*, **1**(4), 689-718.

Paulay, T. [2003] "Seismic displacement capacity of ductile reinforced concrete building systems", *Bulletin of New Zealand Society for Earthquake Engineering*, **36**(1), 47-65.

Paulay, T., Priestley, M.J.N. [1992] *Seismic Design of Reinforced Concrete and Masonry Buildings*, John Wiley and Sons, New York, USA.

Pinto, P.E. (editor) [1997] *Seismic Design of RC Structures for controlled inelastic response*, CEB Bulletin No. 236, Comité Euro-International du Béton, Laussane, Switzerland.

Priestley, M.J.N. [2003] *Myths and Fallacies in Earthquake Engineering, Revisited*, IUSS Press, Pavia, Italy.

Priestley, M.J.N., Calvi, G.M., Kowalsky, M.J. [2007] *Displacement-Based Seismic Design of Structures*, IUSS Press, Pavia, Italy.

Priestley, M.J.N., Grant, D.N. [2005] "Viscous damping for analysis and design", *Journal of Earthquake Engineering*, **9**, Special Edition No. 2.

Priestley, M.J.N., Kowalsky, M.J. [1998] "Aspects of drift and ductility capacity of rectangular cantilever structural walls", *Bulletin, NZ National Society for Earthquake Engineering*, **31**(2), 73-85.

Shibata, A., Sozen, M. [1976] "Substitute structure method for seismic design of reinforced concrete", *Journal of the Structural Division, ASCE*, **102**(1), 1-18.

Sullivan, T., Priestley, M.J.N., Calvi, G.M. [2006] *Seismic Design of Frame-wall Structures*, IUSS Press, University of Pavia, Italy.

Table 1. Trend values of Z/I ratio for some AISC W-shapes.

W-shape group	*Z/I (in^{-1})*	*Z/I (m^{-1})*
W12	0.157	6.19
W14	0.140	5.52
W16	0.136	5.36
W18	0.119	4.67
W21	0.103	4.04
W24	0.087	3.44
W27	0.077	3.04
W30	0.066	2.58
W33	0.072	2.82
W36	0.060	2.35

Table 2. Characteristics of frame-wall structures.

	4 storey	*12 storey*	*20 storey*
Wall length & thickness (m)	4.0x0.35	6.0 x0.35	8.0 x0.35
Inter-storey height (m)	4.0	4.0	4.0
W-beam group, in. (mm)	21 (530)	21 (530)	21 (530)
W-columns group, in. (mm)	14 (360)	14 (360)	14 (360)
Floor seismic weight (kN)	7250	7250	7250

Table 3. Yield and design displacements of the 12 storey building.

Storey	h_i *(m)*	Δ_{iy}	Δ_i	Δ_i^2	$\Delta_i h_i$	$\mu_{Frame,i}$
1	4	0.01	0.06	0.00	0.23	0.84
2	8	0.02	0.13	0.02	1.01	0.98
3	12	0.04	0.20	0.04	2.43	1.09
4	16	0.07	0.28	0.08	4.55	1.18
5	20	0.10	0.37	0.14	7.44	1.26
6	24	0.14	0.46	0.21	11.12	1.31
7	28	0.18	0.56	0.31	15.59	1.34
8	32	0.22	0.65	0.42	20.84	1.36
9	36	0.26	0.75	0.56	26.85	1.36
10	40	0.31	0.84	0.71	33.62	1.36
11	44	0.35	0.94	0.87	41.14	1.36
12	48	0.39	1.03	1.06	49.42	1.36
		Σ=	6.27	4.43	214.25	14.8

Table 4. Intermediate design results for frame-wall structures

	4 storey	***12 storey***	***20 storey***
Proportion of V_b assigned to walls (%)	60	50	45
Frame yield drift, $\theta_{ySteelFrame}$ (%)	1.74	1.74	1.74
Inflection height, h_{inf} (m)	16.0	30.83	46.9
Effective Height, h_{eff} (m)	12.2	34.19	56.43
Design storey drift, θ_d (%)	2.5	2.36	2.19
Design displacement, Δ_d (m)	0.26	0.71	1.06
Wall curvature ductility, μ_{Wall}^{ϕ}	14.28	10.44	7.80
Wall displacement ductility, μ_{Wall}	4.78	2.87	2.22
Average frame ductility, μ_{Frame}	1.28	1.23	1.13
System ductility, μ_{sys}	3.22	2.02	1.60
System damping, ξ_{SDOF}	13.0	10.6	9.0
Effective mass, m_e (t)	2377	6557	10615
Effective period, T_e (s)	1.7	4.1	5.9

Table 5. Final design strengths for frame-wall buildings.

	4 storey	***12 storey***	***20 storey***
Base shear (kN)	9035	10770	12977
Wall strength (kN)	29526	84474	151826
Wall longitudinal reinforcement (%)	1.40	1.62	1.44
Beam section (in×lb/ft)	21×55	21×73	21×93
and strength (kNm)	825	1130	1450
Interior column section (in×lb/ft)	14×132	14×193	14×257
and strength (kNm)	1535	2330	3190
Exterior column section (in×lb/ft)	14×68	14×99	14×132
and strength (kNm)	755	1135	1535

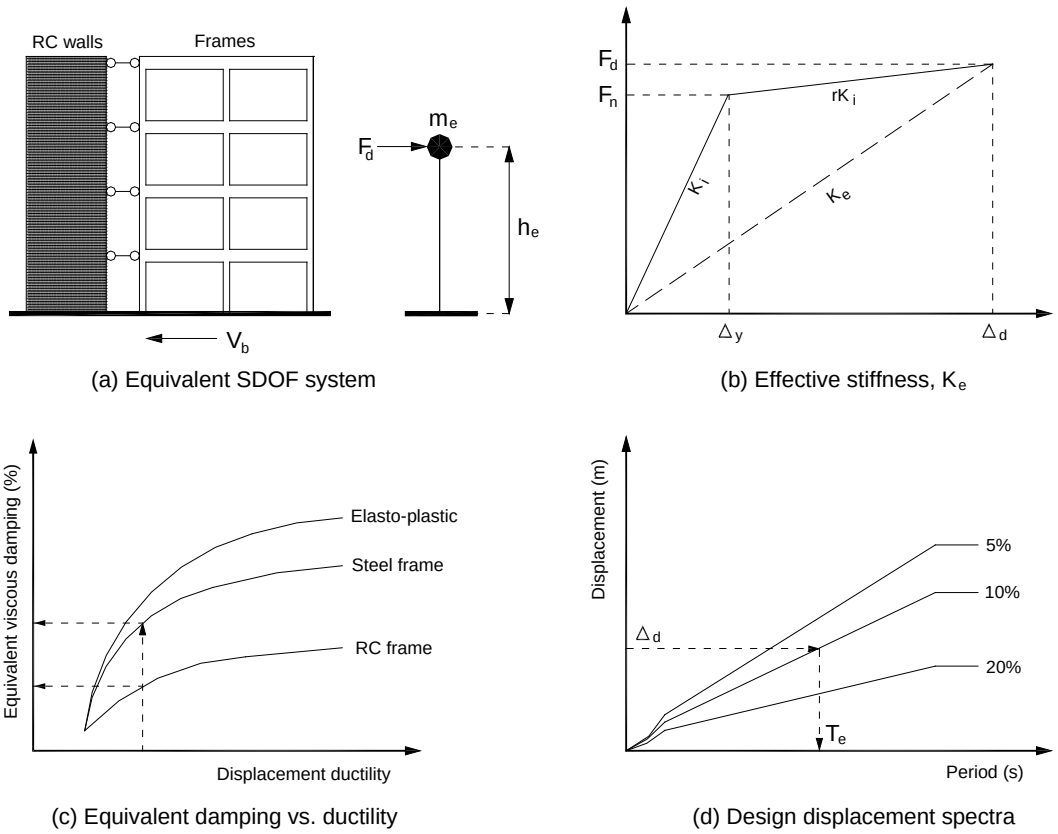

(a) Equivalent SDOF system

(b) Effective stiffness, K_e

(c) Equivalent damping vs. ductility

(d) Design displacement spectra

Fig. 1. Fundamentals of Direct Displacement Based Design [adapted from Priestley *et al*, 2007]

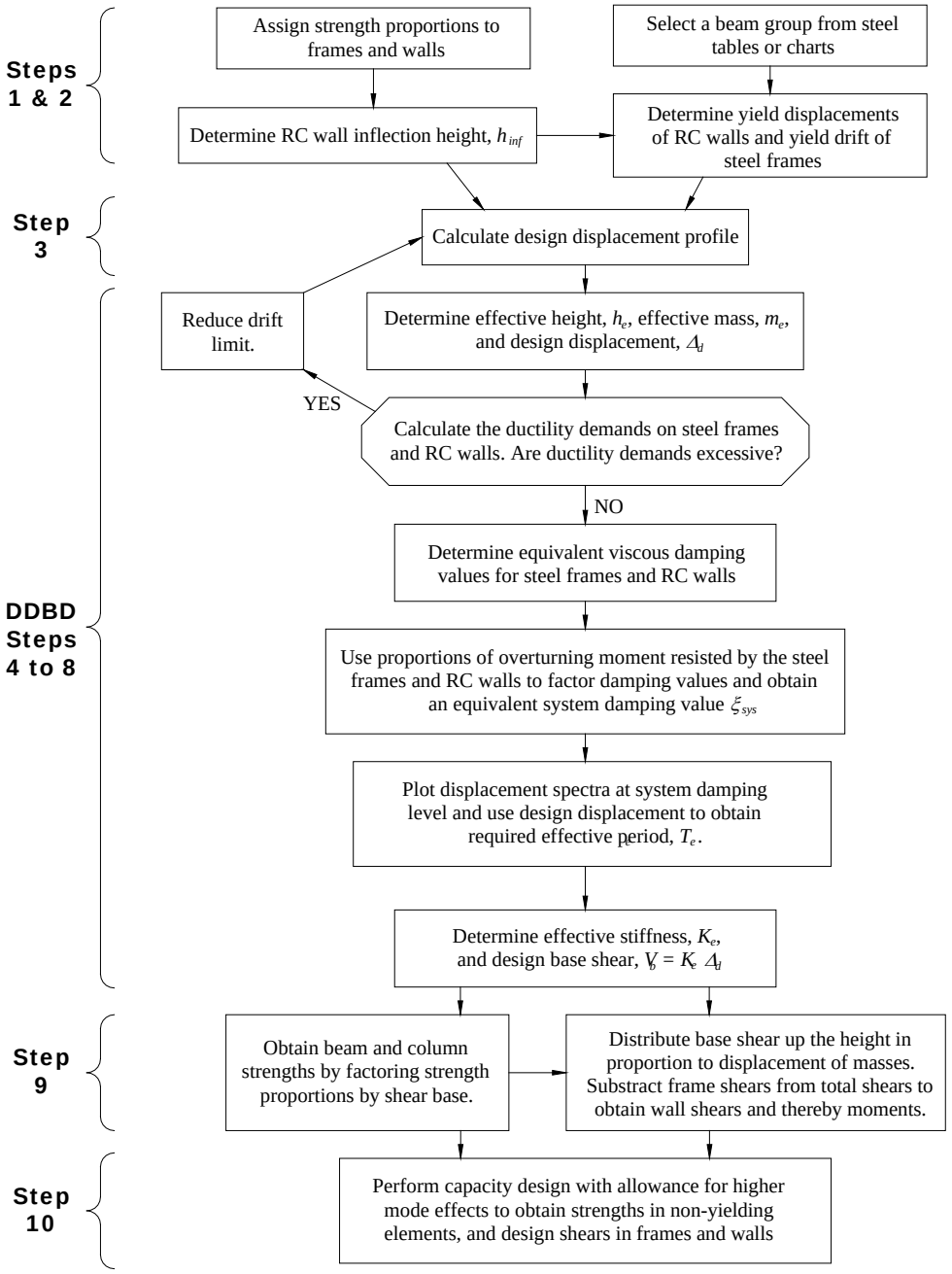

Fig. 2. Flowchart of DBD for dual systems [adapted from Sullivan *et al*, 2006]

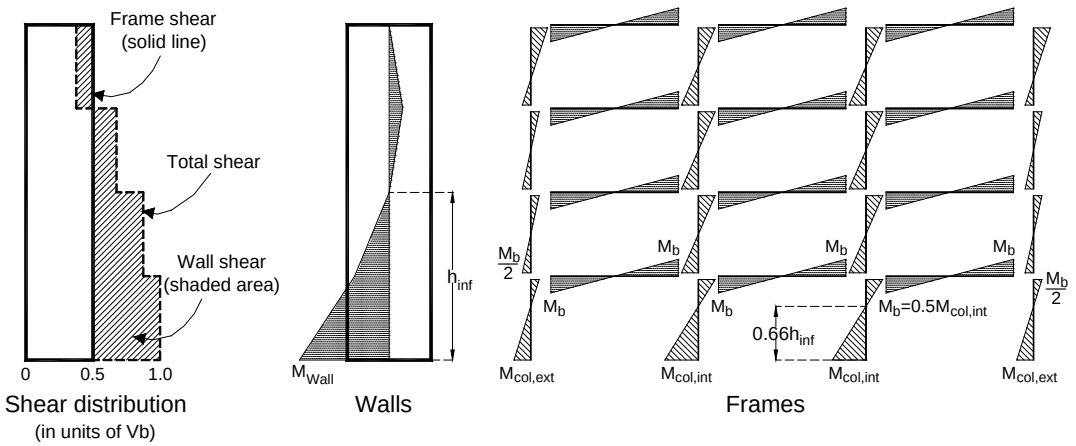

Fig. 3. Shear (left) and moment (right) distribution in frame-wall structures.

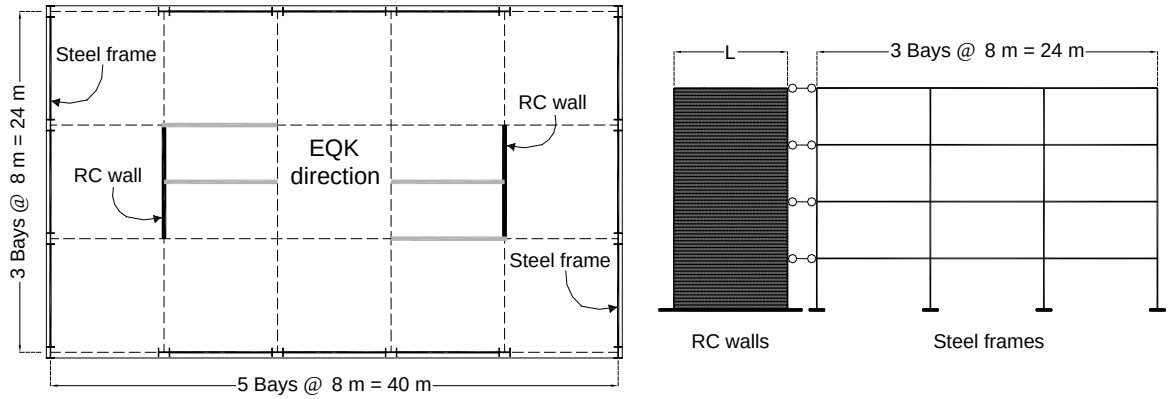

Fig. 4. Geometry of frame-wall structures used in the evaluation.

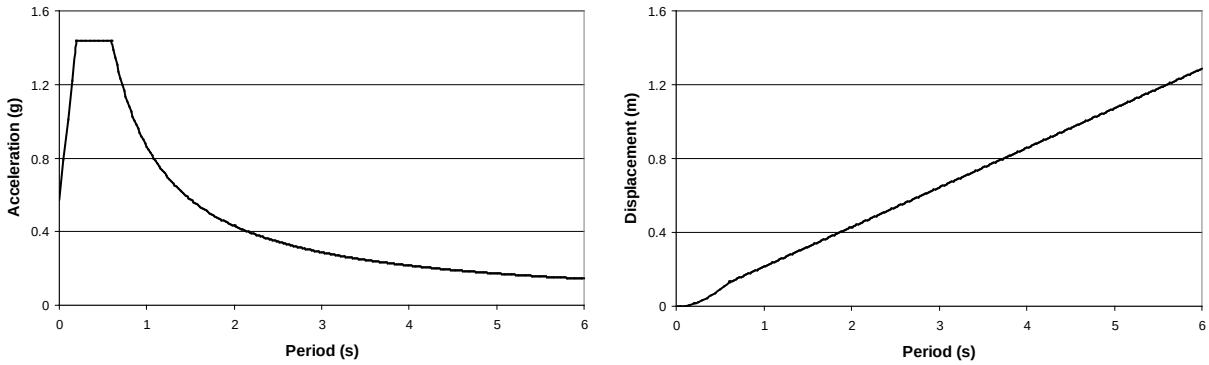

Fig. 5. Design spectrum (left) and displacement design spectrum (right) for 5% of elastic damping.

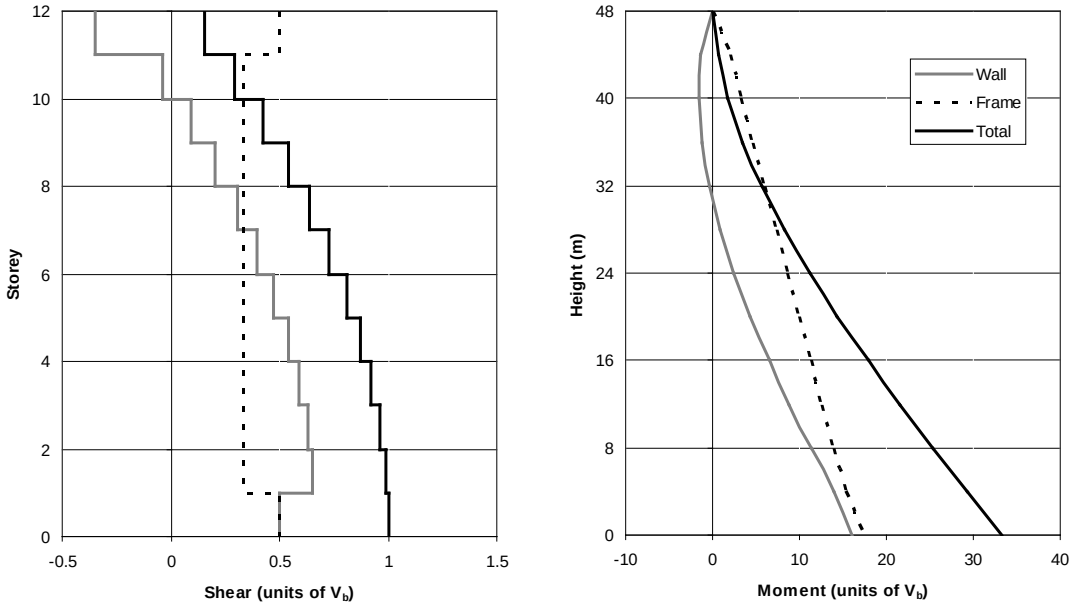

Fig. 6. Shear (left) and moment (right) profiles for the 12 storey frame-wall structure.

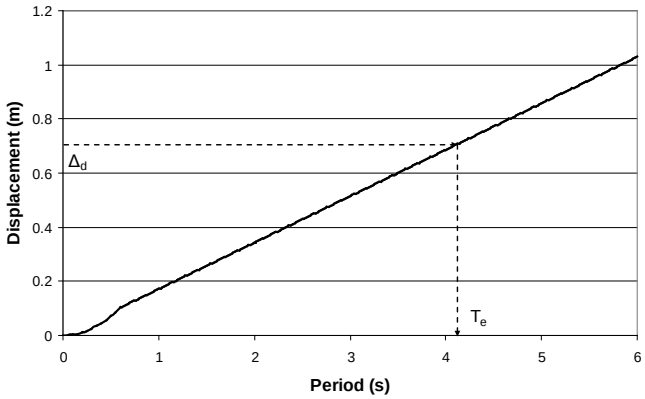

Fig. 7. Displacement design spectrum for ξ_{sys}=10.6%.

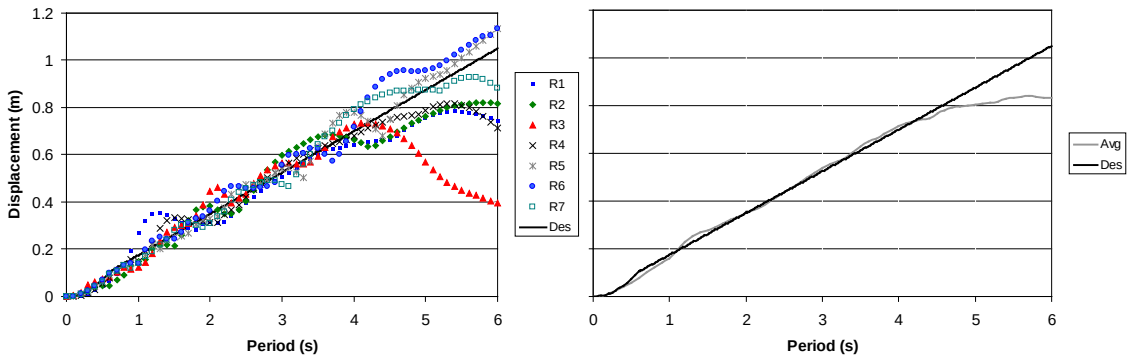

Fig. 8. Displacement design spectrum (left) and fitting of artificial records (right) for an elastic viscous damping of 10%.

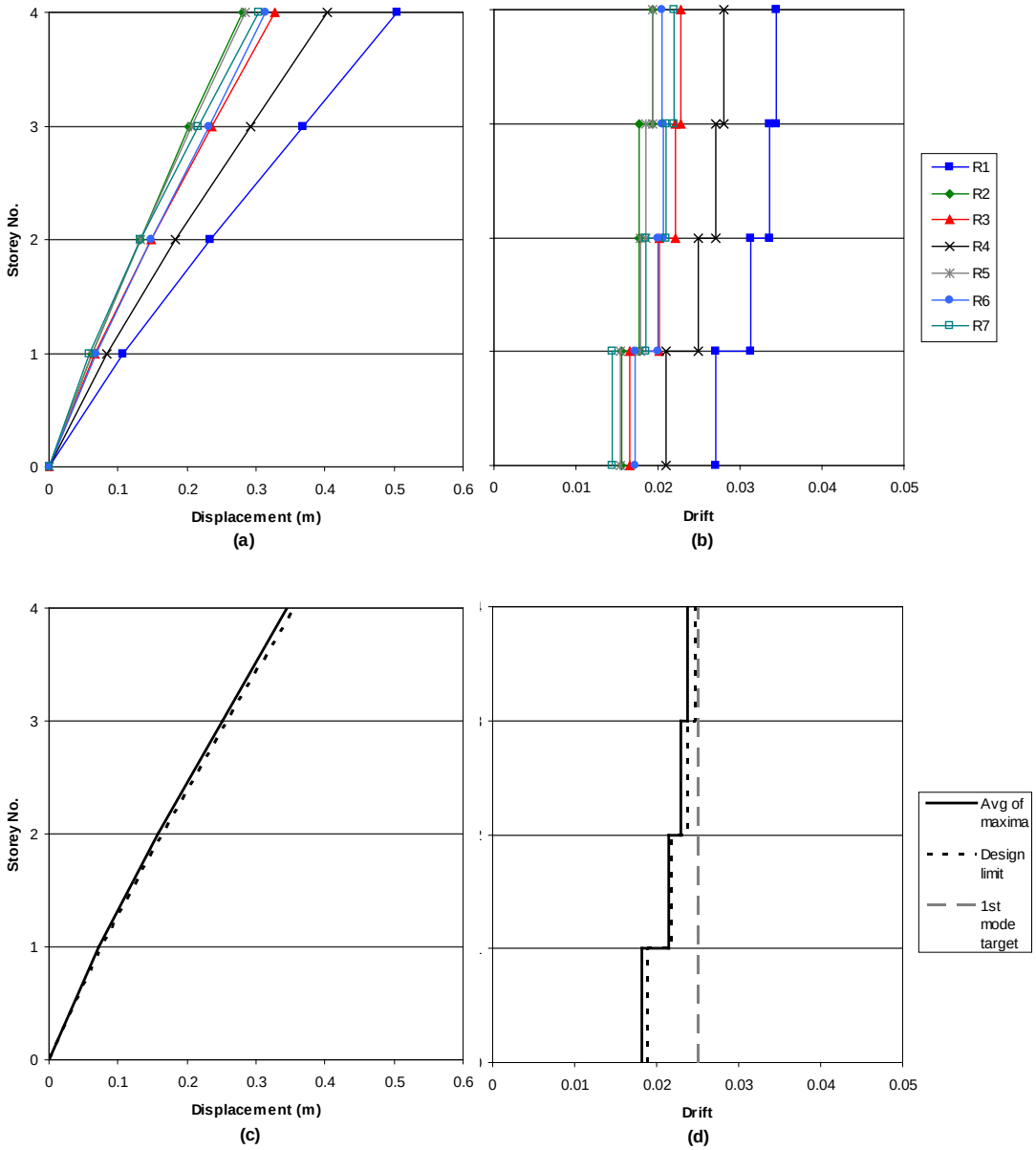

Fig. 9. Results for 4 storey structure: (a) maximum displacements and (b) drifts from time-history, (c) average of the maximum displacements, and (d) average of maximum drift vs design and 1st mode target (2.5%) drift.

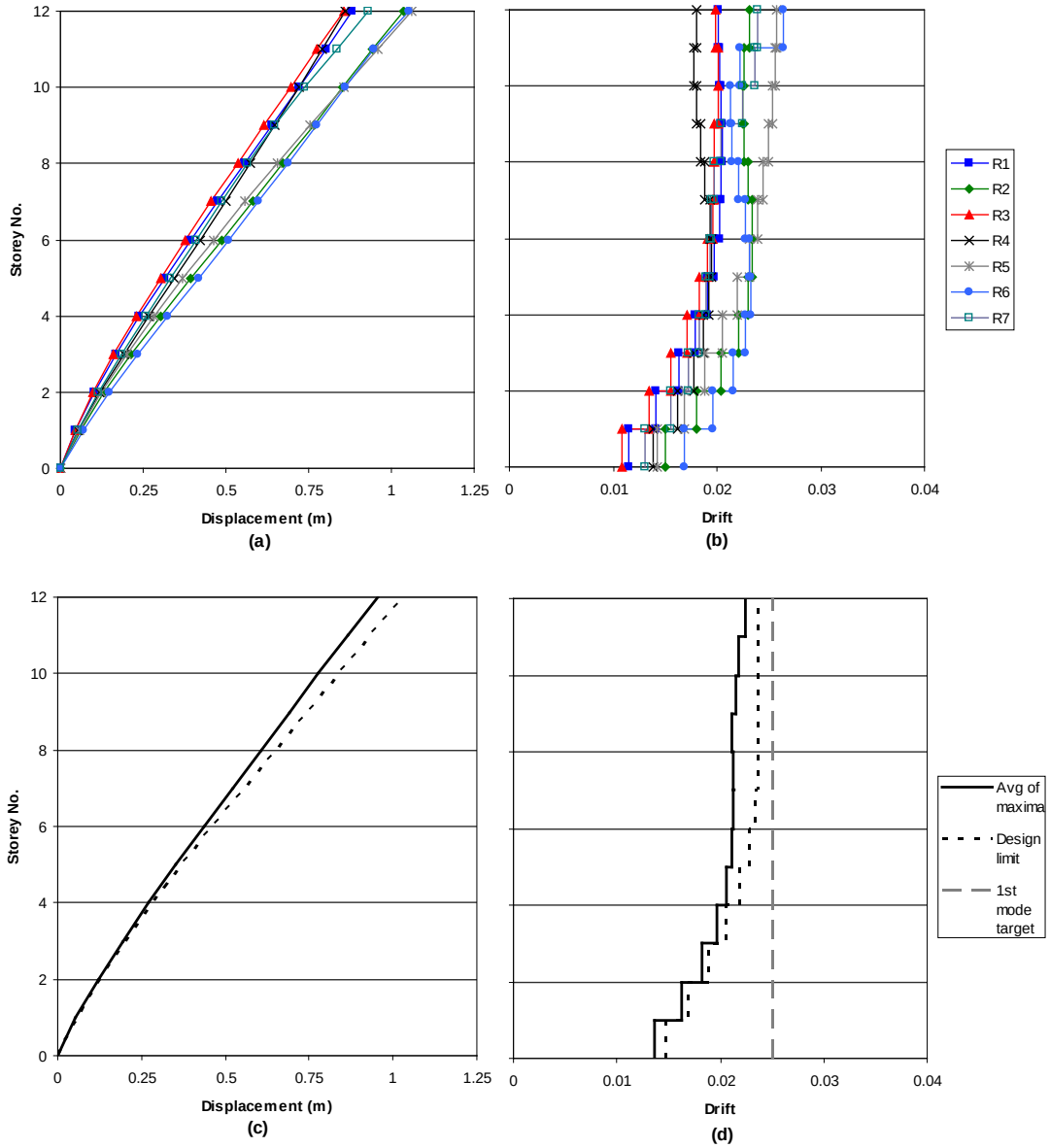

Fig. 10. Results for 12 storey structure: (a) maximum displacements and (b) drifts from time-history, (c) average of the maximum displacements, and (d) average of maximum drift vs design and 1st mode target (2.5%) drift.

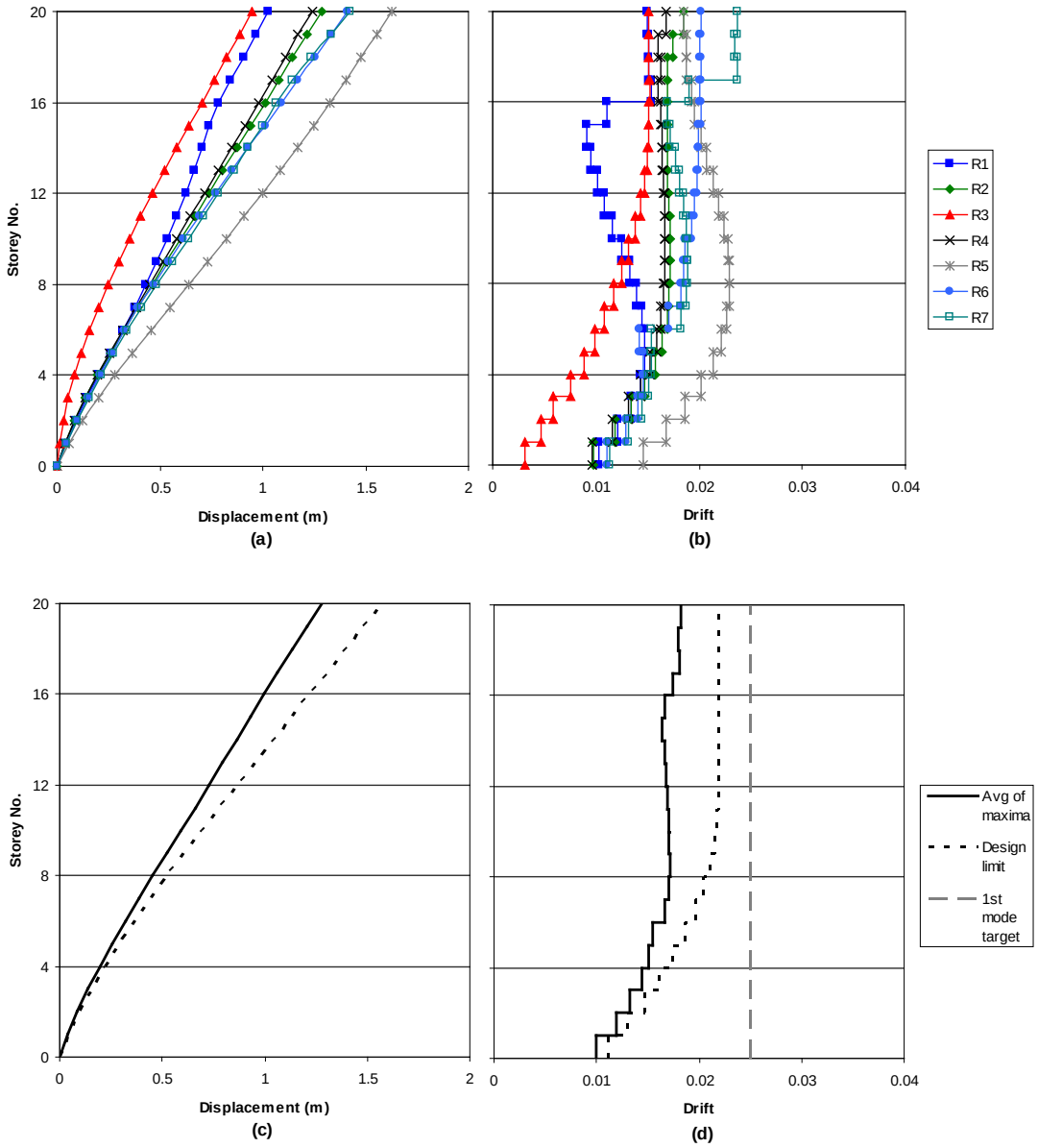

Fig. 11. Results for 20 storey structure: (a) maximum displacements and (b) drifts from time-history, (c) average of the maximum displacements, and (d) average of maximum drift vs. design and 1st mode target (2.5%) drift.